Numerical simulations of the random phase sine–Gordon model and renormalization group predictions.

David Lancaster[1]
J. J. Luiz-Lorenzo[2]

[1] Harrow School of Computer Science, University of Westminster,
[2] Depto. de F´ısica, Facultad de Ciencias, Universidad de Extremadura

This is an electronic version of an article published in the Journal of Statistical Mechanics, (2007) P01003 doi:10.1088/1742-5468/2007/01/P01003.

Numerical Simulations of Random Phase Sine-Gordon Model and Renormalisation Group Predictions

D. J. Lancaster[1] and J. J. Ruiz-Lorenzo[2]

[1] *Department of Computer Science, Westminster University, London, UK*[*]
[2] *Depto. de Física, Facultad de Ciencias, Universidad de Extremadura, 06071 Badajoz, Spain. Instituto de Biocomputación y Física de los Sistemas Complejos (BIFI).*[†]

(Dated: November 1, 2006)

Numerical Simulations of the random phase sine-Gordon model suffer from strong finite size effects preventing the non-Gaussian $\log^2 r$ component of the spatial correlator from following the universal infinite volume prediction. We show that a finite size prediction based on perturbative Renormalisation Group (RG) arguments agrees well with new high precision simulations for small coupling and close to the critical temperature.

PACS numbers: 68.35.Ct, 68.35.Rh, 05.70.Np, 74.25.Qt

I. INTRODUCTION

The random phase sine-Gordon model plays a role in understanding a variety of phenomena. The model has been physically interpreted in terms of roughening of crystalline surfaces [1], pinning of flux lines in superconducting film [2–7] charge density waves [8, 9], and other systems. The model has generated a variety of theoretical predictions [1, 5, 10], not all in agreement, and continues to be a scene of activity [11–14]. Numerical simulations [13–21] might be expected to play a decisive role in this situation, but this has not in fact been the case. Over the past few years, some of the differences between simulations and theory have been resolved as a result of better simulations and analysis [16, 17] and corrections to the precise values of theoretical predictions [22, 23], but there still remain discrepancies.

The primary discrepancy between theory and simulation concerns the presence of a $\log^2 r$ component of the spatial propagator computed at distance r in the *high* temperature phase (since the high temperature phase is Gaussian, the spatial correlator should be simply $\log r$). In the renormalisation group (RG) approach, this component is expected below the critical temperature at length scales beyond a characteristic length that diverges as the critical temperature is approached from below. However, in finite lattice simulations, this component is observed [18] above the expected critical temperature, depending on the strength of the disorder, and leads to uncertainty in actually identifying the location of the critical point [13]. Although the possibility that the critical temperature could depend on the strength of the disorder was raised in theoretical work [24], the accepted theoretical view is that this does not occur. The reason for this is a symmetry of the Hamiltonian, noted by Cardy and Ostlund [25] and recognised as a particular example of the so-called statistical tilt symmetry [26]. Another discrepancy concerns the strength of the $\log^2 r$ component in the *low* temperature phase. The RG prediction for this strength turns out to be universal, yet it does not match the value observed in simulations on achievable lattice sizes. Figure (1) illustrates the discrepancies between the infinite volume RG prediction and data from simulations of several years ago [18]. These phenomena have been observed in other numerical studies [13].

In this paper we use perturbative RG arguments to estimate the size of the $\log^2 r$ component for small couplings in the vicinity of the critical temperature bearing in mind the finite size of the lattices used in simulation. We confront these estimates with data from new high precision simulations made within the restricted parameter range where perturbation theory can be relied upon. Our estimates *do* display a $\log^2 r$ behaviour above the critical temperature and match the strength below the critical temperature therefore resolving the discrepancy.

To use the RG theory to make predictions on the lattice, we need to compute the coefficients appearing in the RG equations using a lattice regulator. The usual treatment is via a Coulomb gas [25] which involves a completely different type of regulator. We have obtained RG coefficients for the lattice regulator by adapting Kogut's original approach of momentum shell integration [27]. These coefficients are substantially smaller than the conventional Coulomb gas ones, and allow quantitative agreement with the simulation data. Nonetheless, the RG theory is only valid for small couplings, and only in this region do we obtain good agreement.

[*]Electronic address: D.J.Lancaster@westminster.ac.uk
[†]Electronic address: ruiz@unex.es

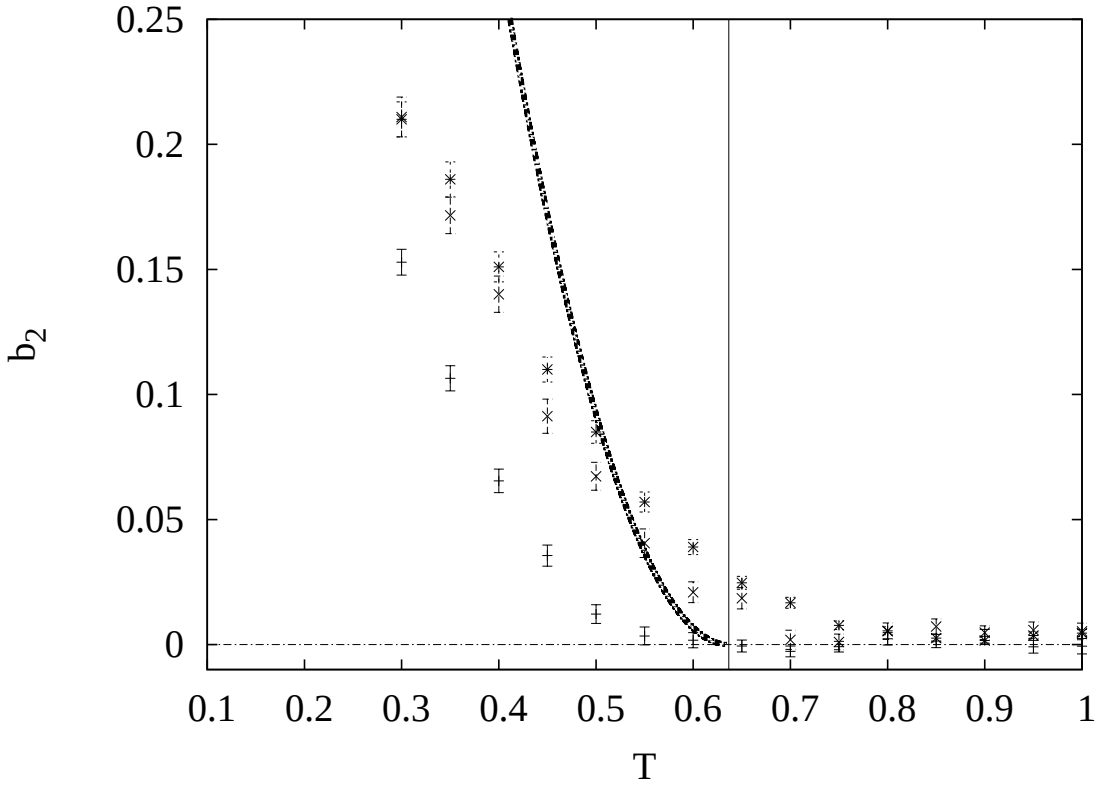

FIG. 1: Numerical results for the coefficient b_2 (see the text) of the $\log^2 r$ term in the correlator on a 64^2 lattice using data originally discussed in [17, 18]. Bottom to top: $\lambda = 0.5, 2.0$ and the discrete height model (formally equivalent to the sine Gordon model with $\lambda = \infty$). The vertical line indicates the position of the infinite volume critical temperature at $T_c = 2/\pi$, and the horizontal line shows $b_2 = 0$. The wider line marks the (universal) infinite volume RG prediction ($b_2 = 2\tau^2$).

We commence with a description of the model and simulation data we wish to explain but relegate technical details of numerical work to appendix A. Then in section III, we briefly review the RG for this model and refer to appendix B for the full computation of RG coefficients appropriate to the lattice regulator. Section IV discusses our technique for estimating the finite size correlator and presents results in the form of a figure confronting the prediction against the new simulation data. The conclusion critically discusses our treatment and since this work does not constitute a full finite size theory, it also discusses some of the issues involved in such a theory.

II. SIMULATIONS

The random phase sine-Gordon model has Hamiltonian,

$$H = \sum (\phi_i - \phi_j)^2 - \lambda \sum \cos 2\pi(\phi_i - \eta_i)\,. \tag{1}$$

Depending on the physical system, the continuous field ϕ may be interpreted in different ways. In the case of a surface, ϕ is the height of the interface so the field ϕ is not periodic and vortices are excluded. The disorder is contained in the term η which is characterised by some probability distribution. Usually a flat distribution for the quenched disorder in $0 \leq \eta < 1$, is assumed, but other distributions have also been simulated [13].

In order to clarify the problems that arise in simulations, let us start by recalling the results of our earlier numerical study [18] of this model which form the basis of figure (1). Signals of a transition were clear in both the static and dynamic properties [38]. Although the static correlation function had the expected $\log r$ behaviour for high temperature, it was clear that another component was present at low temperatures. The results were not sufficiently sensitive to determine the functional form of this additional component, but a $\log^2 r$ term as predicted by the RG studies allowed a good fit to the data. To be precise, the simulated spatial correlator was fitted with the function

(using $\langle(\cdots)\rangle$ to denote average over the thermal noise and $\overline{(\cdots)}$ as the average over the quenched disorder):

$$G(r) \equiv \overline{\langle(\phi_r - \phi_0)^2\rangle} = b_1 P_L(r) + b_2 P_L^2(r) \tag{2}$$

b_1 and b_2 are the fit parameters and $P_L(r)$ is the Gaussian correlator on a lattice of size L,

$$P_L(r) = \frac{1}{2L^2}\sum_{n_1=1}^{L-1}\sum_{n_2=0}^{L-1}\frac{1-\cos(\frac{2\pi r n_1}{L})}{2-\cos(\frac{2\pi n_1}{L})-\cos(\frac{2\pi n_2}{L})} \simeq \frac{1}{2\pi}\log(2\sqrt{2}e^{\gamma_E}r)\,, \tag{3}$$

and the symbol $\simeq$ holds for large lattices, $L \gg 1$ and length scales, r, that are large but not approaching L. γ_E is the Euler-Mascheroni constant. This is actually the correlator along a lattice axis and is the appropriate quantity to compare with the correlators obtained from simulation.

Instead of relying on our old data to make comparison with our predictions we have performed new high precision simulations. These new simulations at small coupling, $\lambda = 0.5$, remain on the same 64^2 lattice but have better thermalization, an improved random number generator and higher statistics. Details of the simulations and comparison with the old data are discussed in Appendix A along with additional data exploring other values of λ. Data for the coefficient b_2 of the $\log^2 r$ term based on new simulations are presented in figure (3) later in the paper.

III. RENORMALISATION GROUP

A convenient basis for the RG studies is the continuum replicated version of the Hamiltonian (1) following Cardy and Ostlund [25]:

$$\beta H = \int d^2x\,\frac{1}{2}\sum_{\alpha\beta} K_{\alpha\beta}\partial\phi_\alpha\partial\phi_\beta - \frac{g}{a^2}\sum_{\alpha\beta}\cos 2\pi(\phi_\alpha - \phi_\beta)\,. \tag{4}$$

Greek letters denote the n replica indices and we have made g dimensionless by explicitly writing the UV cutoff a.

The kinetic term of the replicated Hamiltonian is parameterised with separate coefficients for the on and off-diagonal pieces, $K_{\alpha\beta} = K\delta_{\alpha\beta} + (K - \tilde{K})(1 - \delta_{\alpha\beta})$, since the off-diagonal piece appears after renormalisation even if not present initially. The bare Hamiltonian only has a diagonal term, so the bare parameters are: $\tilde{K}(0) = K(0) = 2\beta$. The bare value of g is related to the parameters of the simulated Hamiltonian by: $g(0) = (\beta\lambda/2)^2$.

RG equations may be obtained from (4) [23, 25, 31–34], though the same results are obtained without replicas [5]. In either case an additional term is generated: in the replica calculation it appears as the off-diagonal part of $K_{\alpha\beta}$, whereas in the other approach it appears as the coefficient of a new term in the Hamiltonian, linear in the derivative of ϕ. These same equations have been derived in a variety of ways; a Coulomb gas approach [25], conventional field theory [31], conformal field theory [33], with the help of the exact renormalisation group [34] and in appendix A, we ourselves use momentum shell integration. Irrespective of the method of derivation, the parameters change with the RG scale, l, in the following way:

$$\frac{dg}{dl} = 2\tau g - Cg^2\,, \tag{5}$$

$$\frac{dK}{dl} = -Ag^2\,, \tag{6}$$

$$\frac{d\tilde{K}}{dl} = 0\,. \tag{7}$$

Where the reduced temperature $\tau = (1 - \tilde{K}_c/\tilde{K}) = (1 - T/T_c)$. The critical temperature is at $T_c = 2/\pi$ (hence, $\tilde{K}_c = \pi$). These perturbative RG equations have been obtained in a double expansion: small coupling g and small reduced temperature τ [31]. They are valid for small couplings in the region near the critical point where higher order terms can be ignored.

The asymptotic form as $l \to \infty$ of the solution of these equations depends on the phase. In the high temperature region where τ is negative, the fixed point value of $g(l)$ is zero and $K(l)$ goes to a constant. In the low temperature region $g(l)$ becomes $g^* = 2\tau/C$, and the coupling $K(l)$ behaves as $K(l) = -4(A/C^2)\tau^2 l$. The consequences of these solutions are fully explored in the literature and we do not repeat the analysis here.

The RG coefficients A, C are dimensionless, non-universal constants of order unity. They depend on the temperature but various workers [5, 31] noted that the amplitude ratio $A/(\tilde{K}C)^2$ appearing in the asymptotic form of $K(l)$ below

T_c, is universal at the critical point. The correct value for this ratio was clarified by Carpentier and Le Doussal [23] (see also reference [22]). In our conventions (note that we keep a factor of 2π inside the cosine term), this ratio is:

$$\frac{A}{(\tilde{K}C)^2} = \frac{R}{(2\pi)^2}\frac{T}{T_c} = \frac{1}{(4\pi)}\frac{T}{T_c}\,. \tag{8}$$

R is the universal ratio defined in [23] and carefully shown to take the value π.

The non-universal values of A and C themselves are necessary to compare with simulation. The regulator natural in the Coulomb gas approach used by Cardy and Ostlund [25] gives values $C = 4\pi$ and $A = 4\pi^3$. These values are rather high and we should properly use values from a lattice regulator. A full perturbative RG computation on the lattice becomes difficult so we have resorted to the following argument.

We have used momentum shell integration following Kogut [27] to rederive the RG equations. This technique needs a modification first pointed out in [35] to take account of the correct operator product expansion, however all computations can be consistently expressed in terms of Gaussian integrals without any need to be concerned with the subtleties of two dimensional massless canonical field theory. Details are given in appendix B, and this technique yields an expression in terms of the Gaussian propagator $< \phi_\alpha(r)\phi_\beta(0) >= K^{-1}_{\alpha\beta}G_0(r)$:

$$C = \frac{8\pi^2}{\tilde{K}}\Lambda^2 \int d^2\xi\, \Lambda \frac{dG_0(\xi)}{d\Lambda} e^{\frac{4\pi^2}{K}[G_0(\xi)-G_0(0)]} = 4\pi e^{\Phi(\infty)}\,. \tag{9}$$

The final expression on the right is evaluated at the critical point, is identical that obtained by a different procedure in [23] and gives the correct value of the universal ratio. Φ depends on the regulation scheme and is defined in terms of the subtracted propagator:

$$[G_0(r) - G_0(0)] = -\frac{1}{2\pi}\log(r\Lambda) + \frac{1}{4\pi}\Phi(r\Lambda)\,. \tag{10}$$

The momentum shell integration technique requires a regulator that is sufficiently smooth to make the term $\frac{dG_0(\xi)}{d\Lambda}$ short range and thus render the expression for C well defined. The lattice propagator has this property, and we can identify $\Phi(\infty)$ using the asymptotic form of the lattice regulator (3) [36]:

$$[G_0(r) - G_0(0)]_{\text{lattice}} \to -\frac{1}{2\pi}\log(r\Lambda 2\sqrt{2}e^{\gamma_E})\,. \tag{11}$$

We therefore use the value of C given by

$$C = \frac{\pi}{2}e^{-2\gamma_E}\,. \tag{12}$$

Recalling the value of the Euler-Mascheroni constant $\gamma_E \simeq 0.577...$, we find this value of C to be substantially smaller than the Coulomb gas value.

IV. FINITE SIZE

In order to compare the RG theory with simulation, we need the correlation function on a finite geometry. The usual derivation of the RG correlator in infinite volume was given by Toner and Vicenzo [1] and we shall proceed in a similar way *without* taking asymptotic values for the RG scale. Numerically it is better to work in the real space, but the fields ϕ do not transform simply under the RG, so we consider the composite fields $e^{iq\phi}$ that have better properties [31]. General RG arguments allow us to write an equation for the correlation function $C_q(r)$ of these vertex operators (see for example reference [31]):

$$C_q(r, \tilde{K}, K(0), g(0)) \equiv \langle \exp\left(iq(\phi(r) - \phi(0))\right)\rangle = \exp\left(-\int_{1/r}^{1}\gamma_q(g(x))\frac{dx}{x}\right) C_q(1, \tilde{K}, K(\log r), g(\log r))\,. \tag{13}$$

Where $\gamma_q(g)$ is twice the (RG) dimension of the vertex operator $\exp(iq\phi(r)$. The leading terms in the perturbative expansion of this quantity are:

$$\gamma_q = \frac{q^2}{2\pi}\frac{1}{\tilde{K}}\left(2 - \frac{K}{\tilde{K}}\right) + \gamma_2(q)g^2\,, \tag{14}$$

Determining the value of γ_2, twice the anomalous dimension, in our RG scheme is not straightforward (it requires the OPE of three vertex operators) and neither has it been computed in other renormalisation schemes. We have therefore only kept the leading term in γ_q when expanding equation (13) in q. We expand to order q^2 and write $C_q(r) = 1 - \frac{q^2}{2}G(r) + O(q^4)$, to obtain an RG equation for $G(r)$:

$$G(r, \tilde{K}, K(0), g(0)) = G(1, \tilde{K}, K(\log r), g = 0) + 2\int_0^{\log(r)} dl \frac{1}{2\pi\tilde{K}} \left(2 - \frac{K(l)}{\tilde{K}}\right) . \tag{15}$$

This expression amounts to using the zeroth order formulae improved with the running coupling constants computed to second order in perturbation theory and is the same procedure usually followed. We will show that this approximation provides us with the same qualitative picture obtained in numerical simulations and a good agreement with the numerical data obtained at small coupling constant. Besides omitting the order g^2 term from the renormalisation factor γ_q, we have consistently terminated the perturbative expansion of G at zeroth order. In fact we have obtained an expression for the order g^2 contribution to G, but the resulting formula is not amenable to numerical calculation on suitable size lattices [39]. We remark that even if we were able to include these order g^2 terms, it would only be a step towards greater precision since the complete model on the lattice also requires irrelevant operators (see appendix C).

On the lattice we replace $\log r$ by its lattice version equation (3), $\log(r) \to 2\pi(P_L(r) - P_L(1))$, so our final equation for the correlator is:

$$G(r, \tilde{K}, K(0), g(0)) = \frac{2}{\tilde{K}} \left(2 - \frac{K\left(2\pi[P_L(r) - P_L(1)]\right)}{\tilde{K}}\right) P_L(1) + 2\int_0^{2\pi(P_L(r)-P_L(1))} dl \frac{1}{2\pi\tilde{K}} \left(2 - \frac{K(l)}{\tilde{K}}\right) . \tag{16}$$

As is the case for the momentum space version, this equation depends on the running coupling $K(l)$ and consequently the behaviour of the correlator depends on the phase. The standard, infinite volume, analysis is based on using the asymptotic solution for $K(l)$. In the high temperature phase where $K(\infty)$ is constant this yields a $\log r$ correlator with the correct coefficient $(T/2\pi)$ even at temperatures beyond the region of validity of the perturbative result. At low temperature the asymptotic solution $K(l) \to -4(A/C^2)\tau^2 l$ leads to the $\log^2 r$ behaviour [1].

$$G(r, \tilde{K}, K(0), g(0)) = 2\tau^2 P_L^2(r) + ... \tag{17}$$

This leading term has universal coefficient, which takes a value $b_2 = 2\tau^2$ (see equation (2)). The sub-leading $\log r$ term, (the dots in the equation above) can be obtained from corrections to the asymptotic value of $K(l)$, though its precise value is dependent on the regulation scheme. Comparison of the two terms yields a length scale that separates the $\log r$ from the $\log^2 r$ behaviour. Since the coefficient of the log does not have any τ factor, this crossover scale diverges as e^{const/τ^2} as T_c is approached from below. This is the problem identified in the Introduction.

To make predictions for finite size, we use the full solution of the RG equation for $K(l)$ [23]:

$$K(l) = K(0) - D\tau \left(\log\left(1 + \chi(e^{2\tau l} - 1)\right) - \chi(1 - \chi)\frac{e^{2\tau l} - 1}{1 + \chi(e^{2\tau l} - 1)}\right) , \tag{18}$$

Where the parameter $\chi = g(0)C/2\tau$ has the same sign as τ. $D = 2A/C^2 = 1/T$, is universal, as discussed in the previous section. This is an exact solution of the perturbative RG equations valid in the region of small $g(l)$, namely for small λ near the transition. By using this expression and numerically solving the real space RG equation (i.e. computing numerically the integral which appears in the right of equation (16)), we are able to compute the finite size lattice correlator $G(r)$. The resulting correlator could be compared directly against simulation data for this quantity, but it is clearer to present the comparison in the same way as we did in our earlier work by fitting the predicted correlator with a form (2).

To put this program in practice we use the value of $C = \pi e^{-2\gamma_E}/2$ that we argued was appropriate for lattice regulation, and we make the fit to the finite size correlator over the range $r = 1, 32$ since both our original and new simulations are on a 64^2 lattice. The resulting predictions are shown in figure (2). These predictions have the same qualitative form as the simulation data shown in figure (1). Namely, we observe the same apparent shift in critical temperature with λ or appearance of $\log^2$ above T_c and the same dependence of this shift, which increases with increasing λ.

For a more precise test of agreement, figure (3) expands the previous figure near the critical temperature to confront the new high precision $\lambda = 0.5$ data against the predictions. The features identified in the Introduction are clearly apparent in the data in figure (3): the continued presence of the $\log^2 r$ coefficient above the expected $T_c = 2/\pi = 0.6366$, and the disagreement with the *universal* infinite volume prediction for this coefficient below T_c. The similarity between the finite size prediction and data is striking. Within the temperature range shown, the

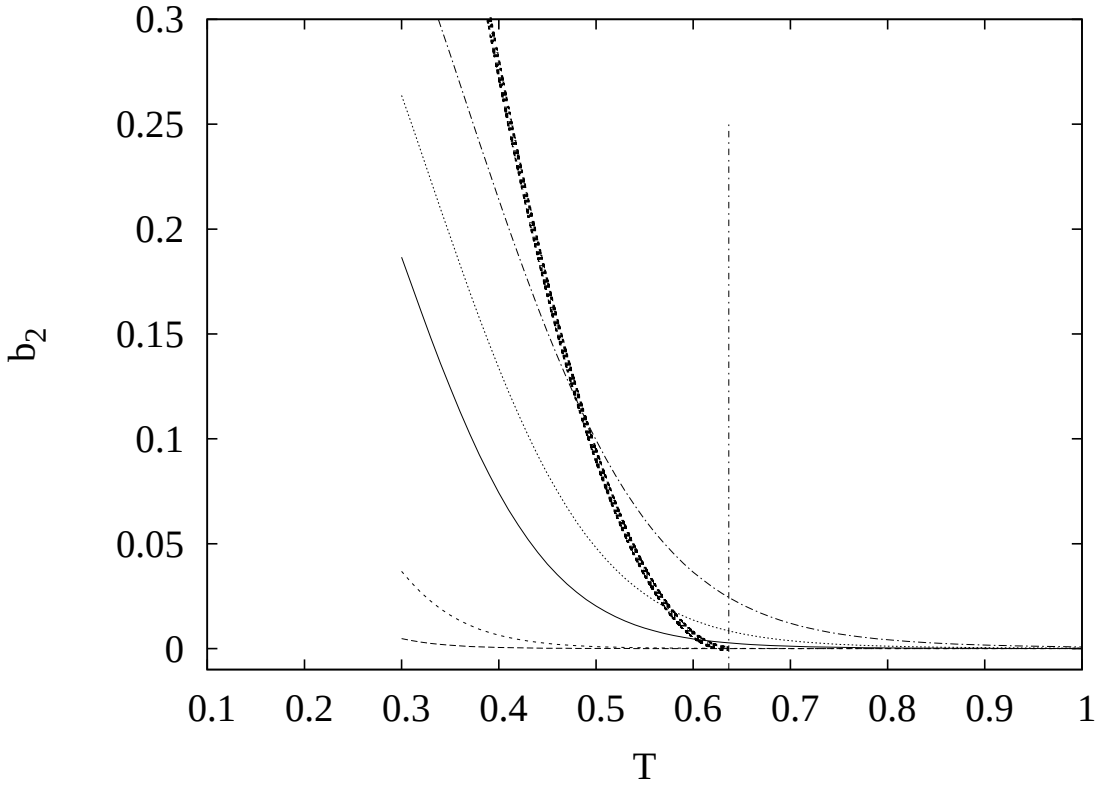

FIG. 2: Theoretical estimate for the coefficient b_2 of the $\log^2 r$ term in the correlator as a function of the temperature as determined by fitting RG predictions for a lattice size 64^2 using the method described in the text. We show continuous lines for five λ values (bottom to top in the plot): 0.1, 0.2, 0.5, 0.7 and 1.0. The vertical line marks the position of the infinite volume critical temperature. The wider line marks the (universal) infinite volume RG prediction ($b_2 = 2\tau^2$).

predictions lie within twice the error bound of the simulations. We can quantify the extent of agreement by computing χ^2 between the numerical data and our theoretical prediction. We obtain $\chi^2 = 5.13$ using the temperatures in the interval $[0.5, 0.7]$, the number of degrees of freedom (d.o.f.) being 5 (notice that we fit the numerical data to a function that we have obtained without resort to these data). The probability to have a χ^2 larger than $\chi^2 = 5.13$ for 5 d.o.f. is 40%, which is larger than the 5% limit typically used in the literature to discriminate the validity of hypotheses [37]. If the interval is enlarged further below the critical temperature to $[0.45, 0.7]$ we obtain $\chi^2 = 7.85$ with 6 d.o.f. corresponding to a probability of 25% [40]. This agreement can also be seen by directly comparing the prediction for the correlator against the result from simulations. At $T = 0.55$ the agreement is very good, with all predicted points lying well within the small errors of the data.

In Appendix A, by way of motivating our choice of parameters for the new simulations, we discuss some exploratory simulations at higher values of λ. These suggest that for larger couplings as we move away from the perturbative regime, the agreement will not be so good. Indeed, in figure (1) the $\lambda = 2.0$ and $\lambda = \infty$ data are not far apart, suggesting that $\lambda = 2.0$ is well into the non-perturbative regime. For these reasons we did not perform any further new simulations. Nonetheless, the predictions in figure (2) retain the qualitative features observed in the original simulations, figure (1).

Although our simulations were only at a particular lattice size, it is illuminating to consider how the results of the procedure above depend on the lattice size. We find that above T_c, as the size is increased, the coefficient b_2 decreases, but the dependence is extremely weak as was found in numerical simulations (in references [17, 18], $L = 64$ and $L = 128$ lattices yielded b_2 curves with overlapping error bars in the low temperature phase). By following our finite size procedure for a range of lattice sizes up to 512, we find a good fit to a scaling form. At $T = 0.7$ the coefficient b_2 goes to zero according to $1/L^{0.39}$ for both $\lambda = 0.5$ and 1.0. This exponent takes a value close to 4τ since at this temperature $\tau = -0.101$. This result corresponds to a finite size dependence $b_2(L) \propto g(L)^2$, that might be expected since g enters the RG equation for K as g^2.

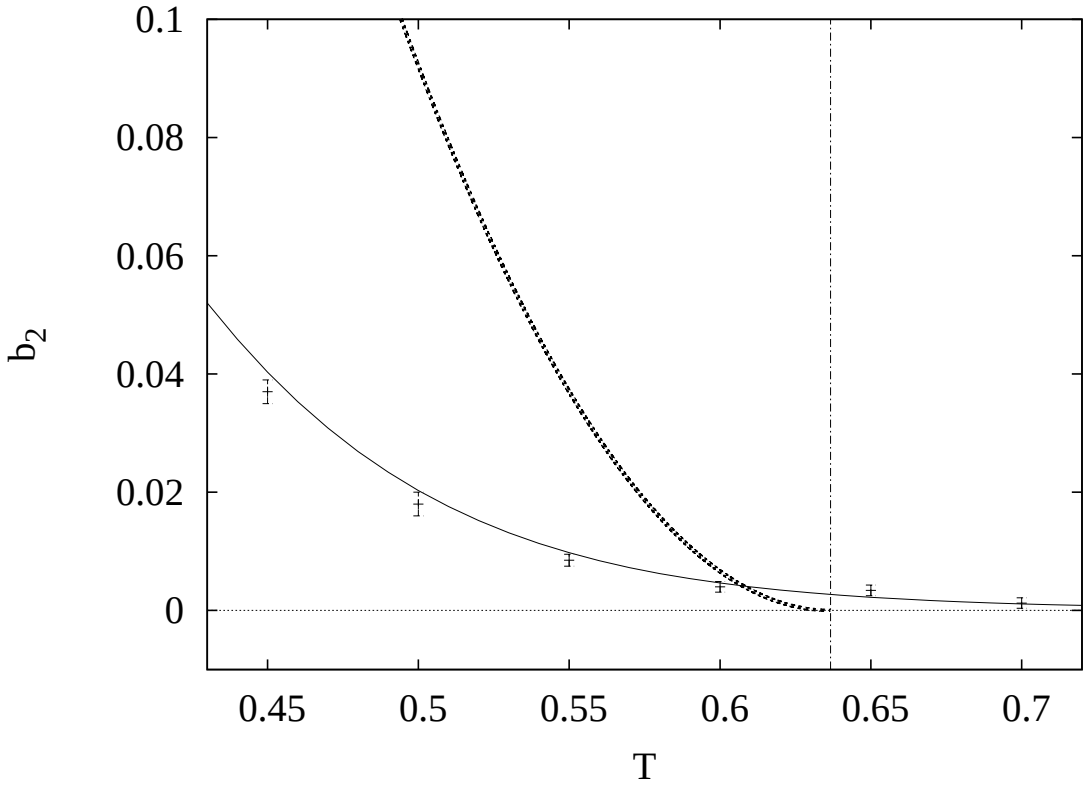

FIG. 3: Comparison of theoretical estimates for the coefficient b_2 of the $\log^2 r$ term in the correlator against new high precision simulations at $\lambda = 0.5$ in the vicinity of the critical temperature. Axes and marked lines have the same significance as in earlier figures. The continuous line is the theoretical estimate for $\lambda = 0.5$ and the points are from the new $\lambda = 0.5$ numerical simulation ($L = 64$).

V. CONCLUSION

Our main result lies in the similarity shown in figure (3) between new simulations and the predictions based on the RG estimate according to our finite size treatment. Until now, the numerical simulation results have been a puzzle since it appears that either there is a $\log^2 r$ component to the correlator above the critical temperature, or that the location of the critical temperature depends on the disorder. Neither of these interpretations are consistent with the conventional RG treatment. In this paper we have shown that one can qualitatively understand the numerical observations in the framework of the RG without the need for any additional ingredient just by taking account of strong finite size effects. Above and near the critical temperature, the disorder strength renormalises to zero and the fixed point is Gaussian. However the dependence on lattice size is extremely slow, and this behaviour induces the $\log^2 r$ term above the critical temperature.

The statistically significant level of agreement relies on several factors. Firstly, the use of new high precision numerical simulations that are better thermalized than the old data. Secondly, the agreement only occurs in the regime where perturbative RG is valid, namely for small disorder strength ($\lambda \leq 0.5$) and near the transition $0.5 \leq T \leq 0.7$. Finally the level of quantitative agreement is crucially dependent on the use of RG coefficients appropriate to the lattice regulator rather than the traditional Coulomb gas values.

Our treatment does not constitute a full finite size theory, and there are several factors we have neglected. The first of these is the perturbative correction from $g(l)$ to the equation (15). Although the leading perturbative contributions to the correlator can be written down, their numerical evaluation would require additional approximations that would undermine attempts to make detailed quantitative comparisons. Moreover, the renormalisation factor from the anomalous dimension of the vertex operator has not been computed. A proper treatment of these perturbative corrections would require a full lattice based perturbative computation. Another factor is the contribution from irrelevant operators. Irrelevant operators can arise from the higher cosine modes after integrating out the disorder and also from the discretisation. A brief discussion of these operators is given in appendix B. A final factor, the use

of an RG coefficient appropriate to the lattice regulator has been included in our treatment, and indeed without this we would not achieve anything like the quantitative agreement shown in figure (3).

In our earlier numerical work [18] we also investigated the dynamics. We found that the dynamical critical exponent z departs from its Gaussian value above the critical temperature, and that the value of this term depends on the disorder strength (see also [14]). We expect that this effect can also be explained in terms of the same strong finite size effects.

Acknowledgements

We wish to thank R. Cuerno, A. Sánchez and A. Sokal for interesting discussions. Partial financial support from CICyT (Spain) grants BFM2003-08532-C03-02 and FISES2004-01399 is acknowledged. We thank A. García for providing computing support.

APPENDIX A: SIMULATION DETAILS

Here we discuss technical details of both the old and new simulations and present additional numerical results. All the data under discussion has been placed in the Journal repository.

1. Original Simulations (dataset A)

Our original numerical simulations [18] were performed in 1995 on an APE supercomputer. Working on a 64^2 lattice, two values of the coupling were considered, $\lambda = 0.5$ and $\lambda = 2.0$ and 128 samples were used for each data point. Figure (1) also shows results for the discrete model [17, 21], but in view of the large coupling this model corresponds to, we do not consider it in the present work.

The data were based on a single annealing run (henceforth called dataset A), with 10^5 thermalization and 2.10^4 measurement sweeps at each temperature (separated by $\Delta T = 0.05$). The random number generator used in this work [28] has since been criticised [29].

2. New Simulations (datasets B,C)

To reduce the size of the error bars on dataset A so as to make quantitative comparisons we performed a number of high precision simulations around the transition temperature. Since the APE machine used for the original simulations is no longer available, we wrote new code running on XEON PC's. These new simulations remain on the same 64^2 lattice but have better thermalization, higher statistics and an improved random number generator (a 64-bit congruential generator based on reference [30]). Both dataset B and C are at $\lambda = 0.5$.

Dataset B checks the new code by using the same parameters and the original annealing schedule of dataset A and closely reproduces those results. Error bars generally overlap, though they are slightly apart at T=0.65,0.7. A χ^2 evaluation gives a confidence limit of 15% that the data arise from the same distribution. The new data (B) tends to give slightly higher signal than the old data (A) and we would ascribe this difference, if significant, to the improved random number generator. We therefore have confidence in the new code.

For improved thermalization, dataset C, the annealing schedule has been lengthened and consists of separate runs of 500 samples with 10^6 thermalization sweeps at temperature intervals of $\Delta T = 0.1$. The final measurements are then taken over 10^6 sweeps. Each data-point (C) lies within two sigma of the other data, however, there is a systematic effect that always increases the new value of b_2 relative to either A or B. Thermalization is the main factor in the difference, but we cannot discount an effect also from the random number generator.

We have also performed runs to observe the approach to thermalization at $T = 0.45$ by tracking the value of the correlator at maximum distance (32, half the lattice size), as the measurements progress. This study indicates that a thermalization of 10^6 sweeps is necessary and sufficient (to an accuracy corresponding to the number of samples we use). We are therefore confident in the new data C and this is what we use in the main text to make quantitative comparisons with the RG predictions.

λ	$b_2^{\rm num}$	$b_2^{\rm th}$
∞	0.085(5)	-
2.0	0.067(6)	0.268
0.7	0.035(2)	0.048
0.6	0.031(2)	0.033
0.5	0.018(2)	0.020
0.4	0.012(1)	0.0105
0.3	0.006(1)	0.0041

TABLE I: Data for b_2 just below T_c at $T = 0.50$. Simulation data (original for $\lambda = \infty, 2.0$ other values from new simulations) denoted by $b_2^{\rm num}$ compared with predictions denoted by $b_2^{\rm th}$.

λ	$b_2^{\rm num}$	$b_2^{\rm th}$
∞	0.025(3)	-
2.0	0.018(4)	0.108
1.0	0.0050(15)	0.020
0.7	0.0046(17)	0.007
0.5	0.0034(9)	0.002

TABLE II: Data for b_2 just above T_c at $T = 0.65$. Simulation data (original for $\lambda = \infty, 2.0$ other values from new simulations) denoted by $b_2^{\rm num}$, compared with predictions denoted by $b_2^{\rm th}$.

3. New Exploratory Simulations

Before deciding the coupling strength to use for run C, we made a short set of new simulations to explore new values of λ at two fixed temperatures: $T = 0.55$ just below T_c and $T = 0.65$ just above T_c.

Table I shows results for a variety of λ just below the critical temperature at $T = 0.50$ (128 samples in each case). At this temperature we are able to make accurate measurements at small λ and have included the data from both new and old simulations. We find that for $\lambda \leq 0.6$ the predictions agree well with the results of the simulations, but at $\lambda = 0.7$ the value is not statistically compatible.

Table II shows similar data, based on 500 samples, for a variety of λ just above T_c at $T = 0.65$. For $\lambda \geq 0.5$ the system shows a clear signal of $\log^2 r$, but we have been unable to obtain statistically useful results for smaller λ due to the number of samples required. We find agreement with predictions at $\lambda = 0.5$, though not at $\lambda = 0.7$, matching the range of agreement just above T_c.

On the basis of the fixed temperature exploratory simulations it appears that $\lambda = 0.5$ is within the range of small coupling where the RG computations are accurate. We therefore collected dataset C at fixed $\lambda = 0.5$ over the temperature range $[0.4, 0.7]$.

APPENDIX B: RG COEFFICIENTS BY MOMENTUM SHELL INTEGRATION

In this appendix we use momentum shell integration technique to derive expressions for the RG coefficients that can be used with a lattice regulator. Although we end up with formulae equivalent to those obtained using other methods in [23], it is only by going through the full derivation that we are able to check that the expressions remain valid with a lattice regulator. The momentum shell technique is direct and intuitive and is an interesting calculation in its own right. The technique is explained by Kogut for the quite similar (ordered) sine-Gordon model in [27]. Since we follow this reference quite closely, in this appendix we only give an outline of the computation with particular details of differences from the ordered sine-Gordon case.

1. Notation

It is convenient to introduce some notation for the local operator:

$$O_{\alpha\beta}(x) = e^{2\pi i(\phi_\alpha(x) - \phi_\beta(x))}\,. \tag{B1}$$

Also for quantities that appear after Gaussian integration.

$$A_{\alpha\beta}(x) = e^{-2\pi^2 G_h(x) K^{-1}_{\alpha\beta}}, \tag{B2}$$

$$B_{\alpha\beta}(x) = e^{-2\pi^2 G(x) K^{-1}_{\alpha\beta}}. \tag{B3}$$

Where $G(x)$ is the full propagator of the ϕ fields and $G_h(x)$ is the propagator for the h fields that have restricted support only in the momentum shell ($\Lambda - d\Lambda < p < \Lambda$).

$$G_h(x) = d\Lambda \frac{dG}{d\Lambda}. \tag{B4}$$

The replica indices only appear through the inverse kinetic matrix and only take distinct values on or off the diagonal. It is therefore useful to write:

$$A(x) = A_{\alpha\beta}(x) \quad \alpha = \beta \text{ (diagonal)}, \tag{B5}$$

$$\tilde{A}(x) = A_{\alpha\beta}(x) \quad \alpha \neq \beta \text{ (off} - \text{diagonal)}. \tag{B6}$$

And similar expressions for B and $\tilde{B}$.

Then, using the explicit expression for $K^{-1}_{\alpha\beta}$, we find a simple form for the combination:

$$A(x)\tilde{A}^{-1}(x) = e^{-2\pi^2 G_h(x)/\tilde{K}}. \tag{B7}$$

In which K does not appear. There is an analogous expression for the B's.

We also define coefficients $b_{\alpha\beta\gamma\delta}(\xi)$ to take account of the connected expectations at second order, given by:

$$b_{\alpha\beta\gamma\delta}(x) = A^2_{\alpha\gamma}(x) A^2_{\beta\delta}(x) A^{-2}_{\alpha\delta}(x) A^{-2}_{\beta\gamma}(x) - 1. \tag{B8}$$

2. Expectations

The change in action as fields (denoted as h) in the momentum shell are integrated out is evaluated perturbatively in g. At first order the Gaussian integration yields the intuitive contractions:

$$\begin{aligned}\langle \cos 2\pi(\phi_\alpha(x) - \phi_\beta(x) + h_\alpha(x) - h_\beta(x))\rangle &= \frac{1}{2}\left(O_{\alpha\beta}(x)\langle e^{2\pi i(h_\alpha(x) - h_\beta(x))}\rangle + \text{c.c.}\right) \\ &= A^2(0)\tilde{A}^2(0)\cos 2\pi(\phi_\alpha(x) - \phi_\beta(x)).\end{aligned} \tag{B9}$$

The second order term is not much harder. In this and all subsequent computations we do not worry about operator ordering or normal ordering and always follow the consistent prescription of the path integral.

$$\begin{aligned}\langle \cos 2\pi\left(\phi_\alpha(x) - \phi_\beta(x) + h_\alpha(x) - h_\beta(x)\right) \quad & \cos 2\pi\left(\phi_\gamma(y) - \phi_\delta(y) + h_\gamma(y) - h_\delta(y)\right)\rangle_{\text{connected}} \\ &= \frac{1}{2}A^4(0)\tilde{A}^{-4}(0)\left(b_{\alpha\beta\gamma\delta}(\xi)O_{\alpha\beta}(x)O_{\gamma\delta}(y) + \text{c.c.}\right).\end{aligned} \tag{B10}$$

The cosine operators are at different spatial points x and y and we have written the difference: $\xi = x - y$.

The coefficients $b_{\alpha\beta\gamma\delta}(\xi)$ take account of the connected form of the expectation and were defined above. For a smooth cutoff, we expect the $b(\xi)$'s to be short range and allow us to use an operator product expansion (OPE) for $O_{\alpha\beta}(x)O_{\gamma\delta}(y)$. Indeed, the momentum shell approach requires a regulator function that allows this step to proceed. The OPE was not needed in Kogut's work, but as pointed out in [35], is necessary in general.

3. Operator Product Expansion

The relevant terms in the OPE are:

$$O_{\alpha\beta}(x)O_{\gamma\delta}(y) \sim a_1(\xi)\delta_{\alpha\delta}\delta_{\beta\gamma}\left(\partial\phi_\alpha - \partial\phi_\beta\right)^2 + a_2(\xi)\left[\delta_{\alpha\delta}(1 - \delta_{\beta\gamma})O_{\beta\gamma} + \delta_{\beta\gamma}(1 - \delta_{\alpha\delta})O_{\alpha\delta}\right]. \tag{B11}$$

We compute the coefficients a_1 and a_2 consistently by using exactly the same Gaussian integration techniques we have employed throughout the computation.

$$a_1(\xi) = -\pi^2 B^4(0)\tilde{B}^{-4}(0)\xi^2 B^{-4}(\xi)\tilde{B}^4(\xi), \tag{B12}$$

$$a_2(\xi) = B^2(0)\tilde{B}^{-2}(0)B^{-2}(\xi)\tilde{B}^2(\xi). \tag{B13}$$

4. RG coefficients

After rescaling the action, we identify the changes to couplings necessary to preserve the physics, and obtain expressions for the RG coefficients.

$$C = -(n-2)\int d^2\xi\, a_2(\xi)\left[A^{-2}(\xi)\tilde{A}^2(\xi)-1\right] = \frac{8\pi^2}{\tilde{K}}\Lambda^2\int d^2\xi\,\Lambda\frac{dG(\xi)}{d\Lambda}e^{\frac{4\pi^2}{\tilde{K}}[G(\xi)-G(0)]}\,, \tag{B14}$$

$$A = -2\Lambda^4\int d^2\xi\, a_1(\xi)\left[A^{-4}(\xi)\tilde{A}^4(\xi)-1\right] = \frac{16\pi^2}{\tilde{K}}\Lambda^4\int d^2\xi\,\Lambda\frac{dG(\xi)}{d\Lambda}\xi^2 e^{\frac{8\pi^2}{\tilde{K}}[G(\xi)-G(0)]}\,. \tag{B15}$$

Notice that these expressions are in terms of a regulated propagator and that although the raw propagator $G(x)$ is infra-red divergent, the formulae appear in terms of well defined propagators: $\frac{dG(\xi)}{d\Lambda}$ and $G(\xi)-G(0)$.

Having checked that $\frac{dG(\xi)}{d\Lambda}$ is short range for the lattice propagator, we can be confident in using the approach with a lattice regulator.

5. Smooth cutoff and Universality

Recognising that $G(r)-G(0)$ is a function of the combination $r\Lambda$ and that $dG(0)/d\Lambda = 1/2\pi\Lambda$; we can write the $dG(x)/d\Lambda$ part of the RG coefficients as:

$$\frac{dG(x)}{d\Lambda} = \frac{d}{d\Lambda}\left[G(x)-G(0)\right] + \frac{1}{2\pi\Lambda}\,. \tag{B16}$$

Then re-expressing the $d/d\Lambda$ as a $\boldsymbol{x}.\nabla$, the derivative can then be taken to act on the exponential to obtain (in the spherically symmetric case):

$$C = \frac{8\pi^2}{\tilde{K}}\Lambda^2\int d\xi\xi\,\left[1+\frac{\tilde{K}}{2\pi}\xi\frac{d}{d\xi}\right]e^{\frac{4\pi^2}{\tilde{K}}[G(\xi)-G(0)]}\,, \tag{B17}$$

$$A = \frac{16\pi^4}{\tilde{K}}\Lambda^4\int d\xi\xi^3\,\left[1+\frac{\tilde{K}}{4\pi}\xi\frac{d}{d\xi}\right]e^{\frac{8\pi^2}{\tilde{K}}[G(\xi)-G(0)]}\,. \tag{B18}$$

Now, without taking limits of any kind, write the propagator in the exponent in the following form for any value of r.

$$G(r)-G(0) = -\frac{1}{2\pi}\log(r\Lambda) + \frac{1}{4\pi}\Phi(r\Lambda)\,. \tag{B19}$$

This is a definition of Φ which contains all the regulator dependence. For small r, this will appear to be an unhelpful decomposition, since $\Phi(r)$ must contain terms to cancel the singularity in the logarithm. For large r, the logarithm is the leading term and all remaining regulator dependence comes from $\Phi(\infty)$. This $\Phi(\infty)$ is the next to leading term of the asymptotic expansion of the propagator that is merely a constant and is often incorporated into the logarithm.

Evaluating A and C at the critical point ($\tilde{K}_c = \pi$):

$$C = 4\pi\int_0^\infty dx\frac{d}{dx}e^{\Phi(x)} = 4\pi e^{\Phi(\infty)}\,, \tag{B20}$$

$$A = 4\pi^3\int_0^\infty dx\frac{d}{dx}e^{2\Phi(x)} = 4\pi^3 e^{2\Phi(\infty)}\,. \tag{B21}$$

Our expressions for the RG coefficients confirm the universal nature of the ratio, since the regulator dependent pieces contained in $\Phi(\infty)$ cancel in the ratio. Moreover the ratio takes the correct [23] value, $R=\pi$.

APPENDIX C: IRRELEVANT OPERATORS

In the theoretical study of the disordered sine Gordon model one usually picks up only the relevant operators (in the RG sense). However the irrelevant ones can induce scaling corrections which modify the behaviour of the system. The goal of this section is to identify such operators and to show up their influence in the scaling of the numerical observables.

We can identify two main sources of irrelevant operators. The first one is the discrete nature of the model which leads to:

$$\phi(r+a^\mu) = \phi(r) + a\partial_\mu\phi + \frac{1}{2}a^2\partial_\mu\phi + \frac{1}{6}a^3\partial^3_\mu\phi + O(a^4)\,, \tag{C1}$$

where a^μ is the lattice vector with modulus a. Hence, in addition to the original kinetic term in the Hamiltonian $(\partial_\mu\phi)^2$), the following terms appear,

$$g_2\int d^dx\ (\partial^2_\mu\phi)^2 + g_3\int d^dx\ (\partial^3_\mu\phi)^2 + g_4\int d^dx\ (\partial_\mu\phi)(\partial^2_\mu\phi) + g_5\int d^dx\ (\partial_\mu\phi)(\partial^3_\mu\phi) + g_6\int d^dx\ (\partial^2_\mu\phi)(\partial^3_\mu\phi) + O(a^8)\,. \tag{C2}$$

One can compute the RG equations to the leading order for each coupling by simply computing their (momentum) dimensions using the Gaussian Hamiltonian:

$$\frac{dg_i}{dl} = (\dim g_i)\, g_i + ...\,, \tag{C3}$$

with $\dim g_2 = -d$, $\dim g_2 = -d$, $\dim \mathrm{g}_3 = -d-2$, $\dim g_4 = -d+1$, $\dim g_5 = -d$, $\dim g_6 = -d-1$. Their value at the lattice scale L is given by:

$$g_i(L) \sim L^{-\dim g_i}\,. \tag{C4}$$

The second source of irrelevant operators is the disorder average. In this paper we consider a flat distribution for the disorder. In addition to the two replica term, the full disorder average of the model induces couplings with an arbitrary number of replicas. The next to leading terms, with four replica interactions, are:

$$u_1\sum_{abcd}\int d^dx\ \cos 2\pi(\phi_a+\phi_b-\phi_c-\phi_d) + u_2\sum_{abcd}\int d^dx\ \cos 2\pi(\phi_a-\phi_b)\cos 2\pi(\phi_c-\phi_d)\,. \tag{C5}$$

By computing their dimensions with the Gaussian Hamiltonian, one can write the leading order RG equations for u_1 and u_2:

$$\frac{du_i}{dl} = 2(2\tau-1)u_i + ...\,, \tag{C6}$$

Therefore both of them are irrelevant (from) well below the critical temperature. At the critical temperature one should expect scaling corrections proportional to

$$u_i(L) \simeq L^{-2}\,.$$

A similar computation shows that the six replica terms would induce corrections proportional to L^{-4}. In general, an n-replica interaction induces corrections proportional to $L^{-(n-2)}$. Clearly, all these scaling corrections, are much weaker than the leading (two replica) one, $g(L) \simeq L^{-2\tau}$.

---

[1] J. Toner and D. P. Di Vincenzo, Phys. Rev. **B 41**, 632 (1990).
[2] M. P. A. Fisher, Phys. Rev. Lett. **62**, 1415 (1989).
[3] T. Hwa, D. R. Nelson, and V. M. Vinokur, Phys. Rev. B **48** 1167 (1993).
[4] Y. C. Tsai and Y. Shapir, Phys. Rev. Lett. **69**, 1773 (1992).
[5] T. Hwa and D.S. Fisher, Phys. Rev. Lett. **72**, 2466 (1994).
[6] C. Zeng, P. L. Leath, and T. Hwa, Phys. Rev. Lett. **83**, 4860 (1999).
[7] C. A. Bolle et al, Nature **399**, 43 (1999).
[8] H. Fukuyama and P. A. Lee, Phys. Rev. B **17**, 535 (1978).
[9] O. Narayan, D. S. Fisher, Phys. Rev. B **48**, 7030 (1993).
[10] T. Giamarchi and P. Le Doussal, Phys. Rev. Lett. **72**, 1530 (1994).
[11] G. Schehr and P. Le Doussal, Phys. Rev. E **68**, 046101 (2003). G. Schehr and P. Le Doussal, Phys. Rev. Lett. 93, 217201 (2004). G. Schehr and P. Le Doussal, Europhys. Lett. 71(2), 290 (2005).
[12] S. Ares, A. Sánchez and A. R. Bishop, Europhys. Lett. **66**, 552 (2004). S. Ares and A. Sánchez Phys. Rev. E **70**, 061607 (2004).
[13] A. Sánchez, A. R. Bishop and E. Moro, Phys. Rev. E **62**, 3219 (2000).

[14] G. Schehr and H. Rieger. Phys. Rev. B **71**, 184202 (2005).
[15] G. G. Batrouni and T. Hwa, Phys. Rev. Lett. **72**, 4133 (1994).
[16] D. Cule and Y. Shapir, Phys. Rev. Lett. **74**, 114 (1995) and Phys. Rev. B **51**, R3305 (1995).
[17] E. Marinari, R. Monasson, and J. J. Ruiz-Lorenzo, J. Phys. A **28**, 3975 (1995). B. Coluzzi, E. Marinari, and J. J. Ruiz-Lorenzo, J. Phys. A **30**, 3771 (1997).
[18] D. J. Lancaster and J. J. Ruiz-Lorenzo, J. Phys. A **28**, L577 (1995).
[19] H. Rieger, Phys. Rev. Lett. (Comment) **74**, 4964 (1995).
[20] U. Blasum, W. Hochstättler, U. Moll, and H. Rieger, J. Phys. A **29**, L459 (1996). H. Rieger and U. Blasum, Phys. Rev. B **55**, R7394 (1997).
[21] C. Zeng, A. A. Middleton, and Y. Shapir, Phys. Rev. Lett. **77**, 3204 (1996).
[22] T. Nattermann and C. Scheidl, Adv. Phys. **49**, 607 (2000).
[23] D. Carpentier and P. Le Doussal. Phys. Rev. B **55**, 12128 (1997).
[24] J. Kierfeld, J. Phys. I France **5**, 379 (1995).
[25] J. L. Cardy and S. Ostlund, Phys. Rev. **B 25**, 6899 (1982).
[26] U. Schultz, J. Villain, E. Brézin and H. Orland, J.Stat. Phys. **51**, 1 (1988).
[27] J.B. Kogut, Rev. Mod. Phys. **51**, 659 (1979).
[28] G. Parisi and F. Rapuano. Phys. Lett. B 157, 301 (1985).
[29] H. G. Ballesteros, L. A. Fernandez, V. Martin-Mayor, A. Munoz Sudupe, G. Parisi and J. J. Ruiz-Lorenzo. Phys. Lett. B400, 346 (1997).
[30] G. Ossola and A. D. Sokal. Nucl.Phys. B691 259 (2004).
[31] Y.Y Goldschmidt, A. Houghton, Nucl. Phys. B **210**, 155 (1982).
[32] Y.Y. Goldschmidt and B. Schaub, Nucl. Phys. **B251**, 77 (1985).
[33] M. Bauer and D. Bernard, Europhys. Lett. **33**, 255 (1996).
[34] G. Schehr and P. Le Doussal, Phys. Rev. E **68**, 046101 (2003).
[35] H.J.F. Knops and L.W.J. den Ouden, Physica **103A**, 597 (1980).
[36] C. Itzykson and J.M. Drouffe. *Statistical Field Theory* (Cambridge University Press, 1989).
[37] J. Salas and A. D. Sokal, J. Stat. Phys. **98**, 551 (2000). See footnote 14.
[38] In numerical work, correlation functions are the basis for these signals, but Fisher and Hwa [5] pointed out that they are inappropriate for experiment since long range correlations of the disorder can confuse their interpretation and therefore they proposed the sample dependent susceptibility. Experimentally the curves $B(H)$ have been measured [7].
[39] The first order term does not vanish on a finite lattice, but it can be evaluated numerically and its effect is negligible.
[40] We can apply this same procedure to compare the predictions against the original data (dataset A in appendix A). For the 5 d.o.f. interval [0.5,0.7], $\chi^2 = 14.6$ with Prob($\chi^2 > 14.6$) = 2.4% and for the 6 d.o.f. interval [0.45,0.7], $\chi^2 = 13.3$ with Prob($\chi^2 > 13.3$) = 2.1%. The agreement is considerably less significant than with the new data.